

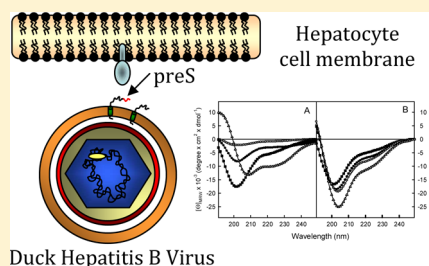
Spectroscopic Characterization and Fusogenic Properties of PreS Domains of Duck Hepatitis B Virus

Carmen L. Delgado,^{†,‡} Elena Núñez,^{†,§} Belén Yélamos,[†] Julián Gómez-Gutiérrez,[†] Darrell L. Peterson,[‡] and Francisco Gavilanes^{*,†}

[†]Departamento de Bioquímica y Biología Molecular, Facultad de Ciencias Químicas, Universidad Complutense, Madrid 28040, Spain

[‡]Department of Biochemistry and Molecular Biology, Medical College of Virginia, Virginia Commonwealth University, Richmond, Virginia 23298, United States

ABSTRACT: In order to shed light on the hepatitis B virus fusion mechanism and to explore the fusogenic capabilities of preS regions, a recombinant duck hepatitis B virus (DHBV) preS protein (DpreS) containing six histidines at the carboxy-terminal end has been obtained. The DpreS domain, which has an open and mostly nonordered conformation as indicated by fluorescence and circular dichroism spectroscopies, has the ability to interact with negatively charged phospholipid vesicles. The observed interaction differences between neutral and acidic phospholipids can be interpreted in terms of an initial ionic interaction between the phospholipid polar headgroup and the protein followed by the insertion of probably the N-terminal region in the cellular membrane. Fluorescence polarization studies detect a decrease of the transition enthalpy together with a small modification of the transition temperature, typical effects of integral membrane proteins. The interaction of the protein with acidic phospholipid vesicles induces aggregation, lipid mixing, and leakage of internal contents, properties that have been ascribed to membrane destabilizing proteins. The fact that the preS domains of the hepadnaviruses have little similarity but share a very similar hydrophobic profile points to the importance of the overall three-dimensional structure as well as to its conformational flexibility and the distribution of polar and apolar amino acids on the expression of their destabilizing properties rather than to a particular amino acid sequence. The results presented herein argue for the involvement of DpreS in the initial steps of DHBV infection. Taken together with previously reported results, the conclusion that both S and preS regions participate in the fusion process of the hepadnaviridae family may be drawn.



Hepatitis B virus (HBV) belongs to the *Hepadnaviridae* family which also includes viruses isolated from mammals (orthohepadnavirus) and birds (avihepadnavirus). All of these viruses are species and cell type specific and show similar genomic organization and replication processes. The study of the initial steps of HBV infection has been difficult due to the lack of a suitable infection system. Even though, in the case of duck hepatitis B virus (DHBV), primary cultures of duck hepatocytes can be infected by DHBV, the entry of DHBV into target cells is still poorly understood. In the past few years it has been postulated that hepadnaviruses enter hepatocytes via endocytic pathways. In the case of DHBV, the carboxypeptidase D, a Golgi-resident protein, has been postulated to be the receptor for avian hepadnaviruses.^{1,2} Because of ubiquitous distribution of this protein, other factors must be involved in host specificity. Thus, the glycine decarboxylase, whose expression is restricted to the liver, kidney, and pancreas that are susceptible to DHBV infection, has been also postulated as a virus receptor.³ Following receptor attachment, DHBV has been shown to take the endocytic route involving early endosomes⁴ or enters the late-endosome compartment.⁵ However, several other receptor candidates able to bind to both S and preS domains have been described for HBV.^{6,7}

In both viral and subviral particles of DHBV, there are two main different surface proteins which are not glycosylated: S,

with 167 amino-acids and 18 kDa, and L, 36 kDa, with an additional 161 amino-acid sequence in the amino-terminal end, the preS domain (DpreS). Both of these proteins are necessary for infection.⁸ A third 10 kDa membrane protein, St, has been observed. This protein consists of the transmembrane fragment 1 of S protein, the internal cysteine loop, and a part of transmembrane fragment 2, which could act as a chaperone for the folding of the L protein.⁹ The preS domain of DHBV envelope protein has been implicated in a wide number of functions in the virus life cycle because of the different topologies that it can adopt. Thus, external DpreS may bind to a putative hepatocyte receptor and induce virus entry into endosomes.¹⁰ Also, it has been postulated that there is a conformational change of L which may be part of the fusion process when the preS domain possesses an intermediate orientation between an internal and external topology.¹¹

Little is known about the role of the different envelope proteins in the viral fusion mechanism. In HBV, a peptide comprising the 16 amino acids at the N-terminus of S protein has been shown to interact with model membranes, promoting liposome destabilization in a pH-dependent manner and

Received: June 22, 2012

Revised: September 26, 2012

Published: September 27, 2012



adopting an extended conformation during the process.^{12,13} The destabilization properties observed for the HBV fusion peptide could be extended to other members of the hepadnavirus family, such as DHBV and woodchuck hepatitis B virus.^{5,14} Evidence for the role of the N-terminal S peptide in fusion has also been obtained by others,^{15,16} who suggest that the exposure of this consensus fusion motif is important in hepadnavirus entry. The HBV preS domain is involved in the fusion of this virus with the plasma membrane of target cells. It was shown to be able to interact in a monomeric way with acidic phospholipid vesicles, to induce aggregation, lipid mixing, and release of internal contents of acidic vesicles resulting in a protein conformational change which increases the helical content.¹⁷ Moreover, a structural motif at the carboxy-terminal end of preS2 has been suggested to be involved in HBV entry,¹⁸ although it seems not to be essential for infectivity.^{19–21} These results suggest that preS could contribute, together with the N-terminal S peptide, to the fusion of viral and cellular membranes.

In order to explore the fusogenic capabilities of DpreS region, a recombinant preS domain from DHBV, produced in *Escherichia coli* cells, was used in membrane interaction studies. In this paper we describe that the preS domain is able to interact mainly with acidic phospholipid vesicles and to destabilize these membrane model systems.

MATERIALS AND METHODS

Reagents. *N*-(7-Nitro-2,1,3-benzoxadiazol-4-yl)-dimyristoylphosphatidylethanolamine (NBD-PE), *N*-(lissamine rhodamine B sulfonyl)-diacylphosphatidylethanolamine (Rh-PE), dimyristoylphosphatidylcholine (DMPC), and dimyristoylphosphatidylglycerol (DMPG) were provided by Avanti Polar Lipids. Egg phosphatidylcholine (PC) and phosphatidylglycerol (PG) were obtained from Sigma. 8-Aminonaphthalene-1,3,6-trisulfonic acid (ANTS), *p*-xylenebis(pyridinium) bromide (DPX), 1,6-diphenyl-1,3,5-hexatriene (DPH), 1-(4-trimethylammoniumphenyl)-6-phenyl-1,3,5-hexatriene (TMA-DPH), and 4-fluoro-7-nitrobenz-2-oxa-1,3-diazole (NBD-F) were purchased from Molecular Probes. Triton X-100 was obtained from Boehringer Mannheim. Sepharose CL-6B Ni-nitrilotriacetic acid (NTA) was purchased from Qiagen. All other reagents were obtained from Merck and Sigma. All solvents were of HPLC grade.

Cloning, Expression, and Purification of DpreS-his Domains. The cloning, expression, and purification processes were similar to those described for the preS domain of HBV²² with some modifications. The preS domain of DHBV was amplified by PCR using DHBV DNA contained in the plasmid pGEM4 DpreS as template and ligated into the pET21b (Novagen) expression vector that adds a six-histidine sequence at the carboxy-terminal end of the protein. The PCR reaction conditions were 1 min at 94 °C, followed by five cycles at 94, 60, and 72 °C, each for 1 min, by 30 cycles at 94, 55, and 72 °C, each for 1 min, and a final “filling in” step at 72 °C for 7 min. The product of the PCR reaction was run on an agarose gel (0.8%), stained with a 1 µg/mL ethidium bromide solution for 15 min, visualized under UV light and extracted using the Qiaex DNA extraction kit (Qiagen). The primers used in the reaction were

DpreS-NdeI(+):

5′ acattt cat ATG GGG CAA CAT CCA GCA AAA

DpreS-EagI(−):

5′ gaaggtac cggccgt TTT CTT CTT CAA GGG

They were designed in such a way that the PCR product had a *NdeI* restriction site (CATATG) at the 5′ end and an *EagI* restriction site (CGGCCG) at the 3′ end (shown underlined). The lowercase letters correspond to the region that hybridize with the plasmid pGEM4-DpreS (DpreS-*NdeI*(+)) or with the S domain (DpreS-*EagI*(−)).

The AmpliTaq-Gold DNA Polymerase (Roche) used adds a dTPA in the 3′ end, so the PCR product was cloned into the linear plasmid pGEM-T (Promega) with 3′ T, then digested with *NdeI* and *EagI* enzymes (New England Biolabs, 10 U/µL) and cloned into the pET21b plasmid, digested with the same enzymes. The cDNA sequence was confirmed by automated DNA sequencing. The resulting plasmid was called pET21b-DpreS.

E. coli strains HMS174 (DE3) or Tuner (Novagen) were transformed with pET21b-DpreS and plated on LB containing 50 µg/mL ampicillin. In these cells, the T7-polymerase gene is under the control of the isopropyl β-D-thiogalactopyranoside (IPTG)-inducible lacUV5 promoter. A single colony was selected and used to inoculate 50 mL of M9 medium supplemented with 0.17% glucose, 1.06 mM MgSO₄, 0.053 mM CaCl₂, and 100 µg/mL ampicillin. Following overnight incubation at 37 °C, the culture was used to inoculate 1 L of fresh M9 medium. This culture was grown to an optical density at 600 nm of 0.6 and then IPTG (Sigma) was added to a final concentration of 0.5 mM and incubated at 30 °C for 4 h, to induce protein expression. The time and temperature of induction were optimized to reduce protein hydrolysis. Cells were harvested by centrifugation at 7400g for 10 min in a GS-3 rotor (Sorvall), and the cell pellet was resuspended in ice cold 10 mM MOPS pH 8.0, 10 mM imidazole, 0.3 M NaCl, 6 M urea. Cells were lysed by tip sonication and centrifuged at 89500g for 30 min in a Beckman SW-28 rotor.

Recombinant protein was purified using a single affinity chromatography step in Sepharose CL-6B Ni-nitrilotriacetic acid (NTA) column (Qiagen) equilibrated with 10 mM MOPS pH 8.0, 10 mM imidazole, 0.3 M NaCl, 6 M urea. DpreS-his recombinant protein was eluted with 10 mM MOPS pH 8.0, 200 mM imidazole, 0.3 M NaCl, 6 M urea. The urea was removed by dialysis against 10 mM MOPS, pH 7.0. The presence of DpreS-his was monitored throughout the purification by SDS-PAGE. Amino acid composition and protein concentration were determined by amino acid analysis performed on a Beckman 6300 automatic analyzer.

Spectroscopic Characterization of DpreS-his. Circular dichroism spectra were recorded on a Jasco J-715 spectropolarimeter equipped with a thermostatted cell. The protein concentration was 0.1 mg/mL (far-UV) or 1 mg/mL (near-UV). The buffer used was 10 mM MOPS pH 7.0. A minimum of three spectra were accumulated for each sample and the contribution of the buffer was subtracted. Values of mean residue ellipticity were calculated on the basis of 110 as the average molecular mass per residue and they are reported in terms of $[\theta]_{\text{M.R.W.}}$ (deg × cm² × dmol^{−1}). The secondary structure of the protein was evaluated by computer fit of the dichroism spectra according to the algorithm convex constraint analysis (CCA).²³ This method relies on an algorithm that calculates the contribution of the secondary structure elements that give rise to the original spectral curve without referring to spectra from model systems.

Fluorescence studies were performed on a SLM Aminco 8000C spectrofluorimeter. The protein concentration was 0.05 mg/mL. The buffer used was 10 mM MOPS pH 7.0. At least three spectra were accumulated and the contribution of the buffer was subtracted. Excitation was performed at a wavelength of 275 or 295 nm, and emission spectra measured over the range of 285–465 nm. The tyrosine contribution to the emission spectra was calculated by subtracting from the emission spectra measured at $\lambda_{\text{exc}} = 275$ nm the emission spectra measured at $\lambda_{\text{exc}} = 295$ nm multiplied by a factor. The factor was obtained from the ratio between the fluorescence intensities measured with $\lambda_{\text{exc}} = 275$ nm and $\lambda_{\text{exc}} = 295$ nm at wavelengths higher than 380 nm, where there is no tyrosine contribution.

Labeling of DpreS-his Domains. Fluorescent labeling of the N-terminus of the protein was achieved following the procedure described by Rapaport and Shai.²⁴ Briefly, DpreS-his protein was incubated at pH 6.8 with a 10 M excess of NBD-F at room temperature for 4 h. Unbound NBD-F was removed by means of a PD-10 column. Labeling of the protein could be monitored by the appearance of a maximum at 467 in the absorbance spectrum, which was used to determine the labeling ratio. The NBD and protein concentrations were determined by using $20000 \text{ M}^{-1} \text{ cm}^{-1}$ as the molar extinction coefficient of NBD-PE and amino acid analysis, respectively.

Vesicle Preparation. In all cases a lipid film was obtained by drying chloroform/methanol (2:1) solution of the lipid under a current of nitrogen and this film was further kept under a vacuum for 4–5 h to completely remove the organic solvent. The phospholipids were resuspended at a concentration of 1 mg/mL in medium buffer (100 mM NaCl, 5 mM MES, 5 mM sodium citrate, 5 mM Tris, 1 mM EDTA) at the appropriate pH value and incubated at 37 °C for 1 h and eventually vigorously vortexed. This suspension was sonicated in a bath sonicator (Branson 1200) for 15 min and was subsequently subjected to 15 cycles of extrusion in a LiposoFast-Basic extruder apparatus (Avestin, Inc.) with 100-nm polycarbonate filters (Costar).

Binding Assay. Binding experiments were conducted as previously described.²⁴ In order to determine the degree of NBD-DpreS-his association with phospholipid vesicles, PC or PG vesicles were added to a fixed amount of labeled protein (0.03–0.06 μM) in medium buffer at the desired pH and incubated at 37 °C for 1–2 min. Fluorescence spectra between 480 and 650 nm were registered in a SLM AMINCO 8000C spectrofluorimeter (SLM Instruments) with excitation wavelength set at 467 nm. A minimum of three spectra were accumulated for each sample. In order to obtain the fluorescence maximum in the presence of lipids, a saturating condition was employed (molar lipid/protein ratio of 4600:1) to avoid the contribution of the free protein to the emission spectrum.

The fluorescence intensity registered at 530 nm at different lipid/protein molar ratios was utilized to obtain the binding isotherm. In order to obtain the partition coefficient, data were analyzed using the equation:

$$X_b = K_p C_f$$

where X_b is the molar ratio of bound protein per total lipid, K_p corresponds to the partition coefficient, and C_f represents the equilibrium concentration of free protein in solution. It was assumed that proteins only partitioned over the outer leaflet of

vesicles. Therefore, X_b values were corrected as $X_b^* = X_b/0.5$ and the data were analyzed as

$$X_b^* = K_p^* C_f$$

Values of the corrected partition coefficient, K_p^* , were determined from the initial slopes of the binding isotherms. In order to calculate X_b , we estimated F_∞ , the fluorescence signal obtained with a saturating phospholipid concentration by extrapolating from a double reciprocal plot of F (total protein fluorescence) versus C_L (total lipid concentration). At every phospholipid concentration, the fraction of bound protein can be calculated by the formula:

$$f_b = (F - F_0)/(F_\infty - F_0)$$

where F_0 represents the fluorescence of unbound protein and F_∞ the fluorescence of bound protein. In all cases, fluorescence from control vesicles in the absence of labeled protein was subtracted. At least three different experiments were performed for each condition.

Fluorescence Polarization. Fluorescence polarization measurements of the probes 1,6-diphenyl-1,3,5-hexatriene (DPH) and 1-(4-trimethylammoniumphenyl)-6-phenyl-1,3,5-hexatriene (TMA-DPH) were taken in the SLM AMINCO 8000C spectrofluorimeter by using 10 mm Glan-Thompson polarizers. DMPG and DMPC vesicles (0.14 mM) were prepared as indicated above containing DPH or TMA-DPH at a weight ratio of 1:500 or 1:100, respectively. The protein-vesicle mixtures were incubated at 37 °C for 30 min. The excitation was set at 365 nm and emission was measured at 425 nm, after equilibration of the samples at the indicated temperature. The temperature in the cuvette was maintained with a circulating water bath. A minimum of three different experiments were performed for each condition tested.

Vesicle Aggregation. The increase in the optical density at 360 nm (ΔA_{360}) produced by addition of DpreS-his protein to a phospholipid vesicle suspension, in medium buffer at the appropriate pH, was measured on a Beckman DU-7 spectrophotometer after incubation at 37 °C for 1 h. Values of control samples containing only vesicles and only protein were subtracted at each protein concentration. The final phospholipid concentration was kept at 60 μM . At least three different experiments were performed for each condition.

Lipid Mixing. Lipid mixing was monitored by using the fluorescent probe dilution assay²⁵ in which the decrease in the efficiency of the fluorescence energy transfer between NBD-PE (energy donor) and Rh-PE (energy acceptor) incorporated into liposomes, as a consequence of lipid mixing, is measured. Liposomes, in medium buffer at the appropriated pH, labeled with 1 mol % NBD-PE and 1 mol % Rh-PE were mixed with unlabeled liposomes in a 1:9 molar ratio. After incubation of liposomes with the DpreS domains at different concentrations at 37 °C for 1 h, emission spectra were recorded with excitation wavelength set at 450 nm. Both the excitation and emission slits were set at 4 mm. The excitation polarizer was kept constant at 90° and the emission polarizer was kept constant at 0° to minimize dispersive interference. The efficiency of the energy transfer was calculated from the ratio of the emission intensities at 530 and 590 nm and the appropriated calibration curve. The final phospholipid concentration was 0.14 mM. The organic solvent itself had no effect on the efficiency of the energy transfer. At least three different experiments were performed for each condition.

Release of Aqueous Contents. Leakage was determined by the ANTS/DPX assay,²⁶ which is based on the dequenching of ANTS fluorescence caused by its dilution upon release of the aqueous contents of one vesicle preparation containing both ANTS and DPX. It was performed by coencapsulating 12.5 mM ANTS and 45 mM DPX in 10 mM Tris, 20 mM NaCl, pH 7.2, in phospholipid vesicles. The lipid film was hydrated as described previously and the vesicles were sonicated for 30 min. Afterward vesicles were subjected to five cycles of freeze–thawing in liquid nitrogen and passed 15 times through a Liposo Fast-Basic extruder apparatus (Avestin, Inc.) with 100-nm polycarbonate filters (Costar). After the vesicles with the coencapsulated probe and quencher were formed, the whole sample was passed through a Sephadex G-75 column (Pharmacia) to separate the vesicles from the non-encapsulated material using medium buffer for elution. Assays were performed at a phospholipid concentration of 0.1–0.14 mM in medium buffer at the appropriated pH, by incubating with different amounts of protein at 37 °C for 1 h and measuring in the SLM Aminco 8000C spectrofluorimeter. The excitation wavelength was set at 385 nm and the ANTS emission was monitored at 520 nm. Both the excitation and emission slits were set at 4 nm. The excitation and emission polarizers were kept constant at 90° and 0°, respectively, to minimize interference due to dispersion. The fluorescence scale was set to 100% by addition of 0.5% Triton X-100, and 0% leakage was obtained measuring the fluorescence of control vesicles without protein. A minimum of three different experiments were performed for each condition tested.

RESULTS

Cloning, Expression, and Purification of DpreS-his.

The cDNA of DpreS-his domain was cloned in the plasmid pET21b at the *Nde*I/*Eag*I sites to yield pET21b-DpreS as described in Materials and Methods. The cDNA sequence was confirmed by automated sequencing.

Plasmid DNA from a colony containing the correct construct was purified and transformed into *E. coli* HMS174 (DE3) cells that were grown and harvested as described under Materials and Methods. Protein expression was induced with IPTG 0.5 mM at 30 °C for 4 h (Figure 1A, lane 3). After the cells were lysed in 10 mM MOPS pH 8.0, 10 mM imidazole, 0.3 M NaCl, 6 M urea, most of the DpreS-his remained in the centrifuged supernatant (Figure 1A, lane 5). This supernatant was applied

to a Ni-NTA column equilibrated with the same buffer. Protein was eluted with 10 mM MOPS pH 8.0, 200 mM imidazole, 0.3 M NaCl, 6 M urea. As it can be observed in Figure 1A, lane 8, the purified protein was partly hydrolyzed. Thus, in order to reduce DpreS-his proteolysis, the plasmid was transformed into Tuner cells (Novagen) and the protein expression was induced with 0.5 mM IPTG at 30 °C for 2 h (Figure 1B). The purification process was carried out under denaturing conditions because it was observed that DpreS-his domains precipitate at concentrations higher than 1 mg/mL. Therefore, after elution, the protein was diluted to approximately 1 mg/mL and dialyzed against 10 mM MOPS pH 7.0 to remove urea. Under these conditions 15–20 mg of highly pure and stable protein were obtained per liter of cell culture (Figure 1B, lane 8).

The protein was shown to be pure by SDS-PAGE, with an electrophoretic mobility close to that expected from its theoretical molecular mass, 19224 Da. The amino acid composition was also indicative of the purity of the protein since it was almost identical to that calculated from the amino acid sequence derived from the DNA sequence (Table 1), taking into account that the cloning strategy added five additional amino acids (TAALE) to the carboxy-terminal end of DpreS just before the six histidine tag.

Table 1. Amino Acid Composition of DpreS-his^a

	theoretic	experimental
Asx	11	11
Thr	12 + 1	12
Ser	7	6
Glx	27 + 1	28
Pro	22	22
Gly	12	12
Ala	8 + 2	10
Val	6	6
Met	3	3
Ile	7	7
Leu	15 + 1	16
Tyr	2	2
Phe	2	2
His	4 + 6	10
Lys	9	9
Arg	9	9
Trp	4	N.D.

^aThe theoretical composition was determined from the amino acid sequence deduced from the cDNA sequence. The experimental composition was determined from the amino acid analysis. The numbers of histidine residues was the sum of the 6xHis tag and the DpreS domain (4). The five amino acids added by the cloning procedure were 1 Thr, 2 Ala, 1 Leu, and 1 Glu. N.D. (not determined).

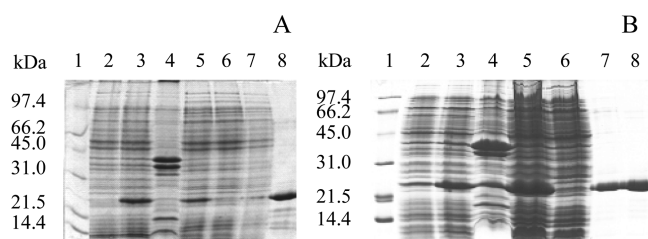


Figure 1. SDS-PAGE of DpreS-his purification steps. *E. coli* HMS174 cells (DE3) (A) and Tuner cells (B) were transformed with pET21b-DpreS. Lane 1, protein markers. Lane 2, transformed cells before induction. Lane 3, transformed cells after 4 h (A) and 2 h (B) IPTG induction. Lane 4, cell pellet. Lane 5, supernatant obtained after disruption of cells in 10 mM Imidazol buffer. Lane 6, protein not retained in the Ni-NTA column. Lane 7, proteins washed from the Ni-NTA column with 10 mM imidazol (A) or 30 mM imidazol (B). Lane 8, pure protein after eluting with 200 mM imidazol buffer.

Spectroscopic Characterization of DpreS-his. The far-UV CD spectrum of the recombinant DpreS-his protein at pH 7.0 is depicted in Figure 2A. It showed a minimum at 200 nm and a shoulder at 220 nm, indicative of a high content of nonordered secondary structure. The assignment of the secondary structure elements according to the algorithm CCA²³ is shown in Table 2. Half of DpreS-his residues are in aperiodic secondary structure, β -sheet being the major repetitive ordered secondary structure component (16%). On the other hand, the positive band observed in the near-UV CD spectra of DpreS-his (Figure 2B) indicates an asymmetric

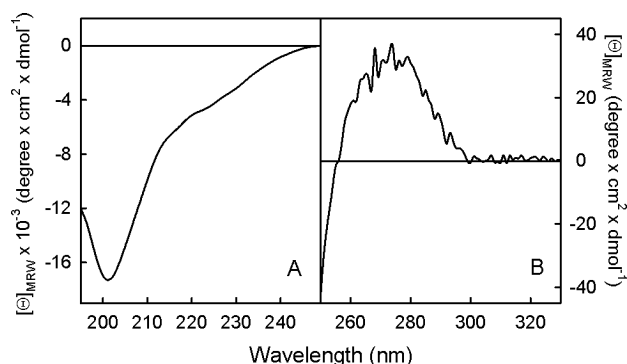


Figure 2. Circular dichroism spectra of DpreS-his. (A) Far-UV CD spectrum. Protein concentration was 0.1 mg/mL and cell path length 0.1 cm. (B) Near-UV CD spectrum. Protein concentration was 1 mg/mL and cell path length was 1 cm. The buffer employed was 10 mM MOPS pH 7.0.

Table 2. Secondary Structure of DpreS-his under Different Conditions Calculated from the CD Spectra According to the CCA Method²³

	secondary structure (%)			
	α -helix	β -sheet	β -turn	aperiodic
DpreS-his, pH 7.0	4	16	29	51
DpreS-his/PG (1:50) pH 7.0	7	0	29	64
DpreS-his/PG (1:50) pH 5.0	30	33	2	35

environment of the aromatic residues of the protein in the three-dimensional structure. The magnitude and the shape of the spectra observed at both pH 7.0 and 5.0 were similar (data not shown).

More information about the three-dimensional structure of the recombinant protein was obtained from the fluorescence emission spectrum (Figure 3). When exciting at either 275 or

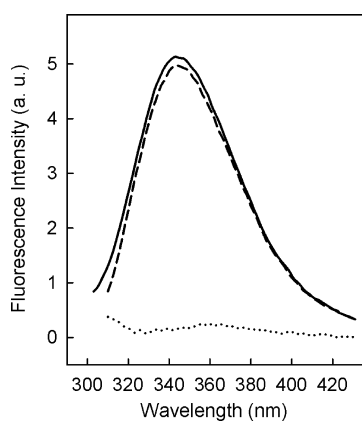


Figure 3. Fluorescence emission spectra of DpreS-his. The protein concentration was 0.05 mg/mL in 10 mM MOPS pH 7.0. The spectra were obtained upon excitation at 275 nm (—) and 295 nm (---). The contribution of tyrosine residues to the emission spectra of the protein (····) is calculated as described in Materials and Methods.

295 nm the recombinant protein exhibited a maximum centered at 344 nm, both at pH 7.0 and 5.0, indicating that all Trp residues are in a highly hydrophilic environment very exposed to the solvent. The tyrosine contribution, calculated as described in Materials and Methods, is almost negligible and very different from that expected for a mixture of Trp and Tyr

in the ratio 4:2 of recombinant DpreS-his, probably due to resonance energy transfer from Tyr residues to nearby Trp residues or to quenching by other nearby amino acids.

Interaction with Phospholipids. Fluorescent labeling of DpreS-his was carried out following the procedure described in Materials and Methods. The extent of labeling was calculated from the absorbance spectrum of NBD-DpreS-his. The reaction with NBD-F resulted in the incorporation of one molecule of NBD to the protein. Taking into account that the reaction was carried out at pH 6.8, it is likely that the α -amino group, and not the Lys side chain, is the main labeling target.²⁴ The emission spectrum of NBD-DpreS-his showed an emission maximum centered at 548 nm, both at pH 7.0 and pH 5.0 (Figure 4), which reflects a hydrophilic environment for the NBD moiety.²⁷

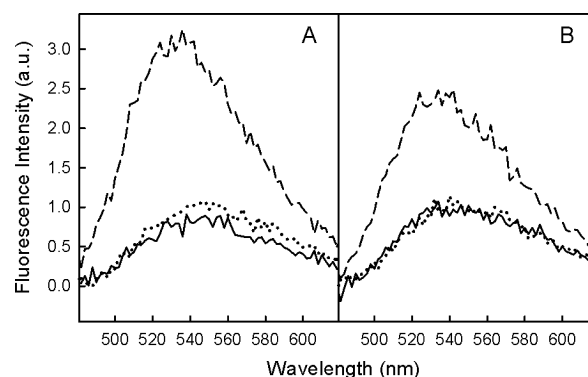


Figure 4. Effect of PG and PC on the fluorescence spectrum of NBD-DpreS-his at pH 5.0 (A) and pH 7.0 (B). Spectrum of NBD-DpreS-his alone (····) and in the presence of PG (---) or PC vesicles (—) at a lipid/protein molar ratio of 4600:1. The excitation wavelength was 467 nm and the protein concentration was 0.03–0.06 μ M.

The position of the fluorescence emission maximum exhibited by the NBD-DpreS-his upon binding to phospholipid vesicles provides information on the relative location of the NBD moiety and hence of the protein N-terminus. Upon interaction with PG vesicles at saturating conditions (molar lipid/protein ratio of 4600:1), to avoid the contribution of the free protein to the emission spectrum, the maximum was shifted to 528 nm, both at pH 5.0 (Figure 4A) and pH 7.0 (Figure 4B), although the increase in fluorescence was lower at neutral pH. The observed blue shift reflects a relocation of the NBD group into a more hydrophobic environment in the presence of negatively charged phospholipids. When neutral phospholipids, PC, were used no changes in the position of the maximum nor in the fluorescence intensity were observed (Figure 4).

In order to calculate the extent of binding, labeled protein at a final concentration of 0.03–0.06 μ M was titrated with increasing amounts of PG or PC vesicles. The mixtures were incubated at 37 °C for 2 min and the fluorescence intensity was measured at 530 nm. The protein concentration was low enough to avoid vesicle aggregation. The measured fluorescence at 530 nm, after subtracting the contribution of control experiments performed by titrating unlabeled proteins with the same vesicle concentration, was plotted against the phospholipid concentration (Figure 5). After incubation with PG, there is a significant increase in the fluorescence intensity either at pH 5.0 (Figure 5A) or pH 7.0 (Figure 5B), with the effect observed at acidic pH being higher. However, after incubation

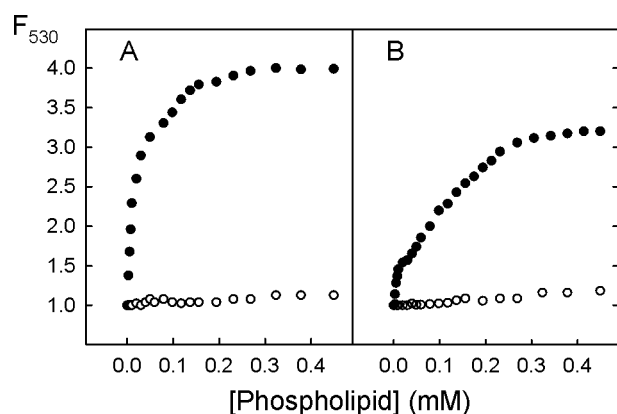


Figure 5. Fluorescence increase at 530 nm of NBD-DpreS-his upon addition of PG (●) or PC vesicles (○) at pH 5.0 (A) or pH 7.0 (B). The excitation wavelength was set at 467 nm. Protein concentration was 0.03–0.06 μ M. The fluorescence values refer to those obtained without lipids.

with PC the increase in fluorescence was almost negligible (Figure 5).

From this data, binding isotherms were obtained (Figure 6). Both at pH 5.0 and pH 7.0 the data showed a nonlinear

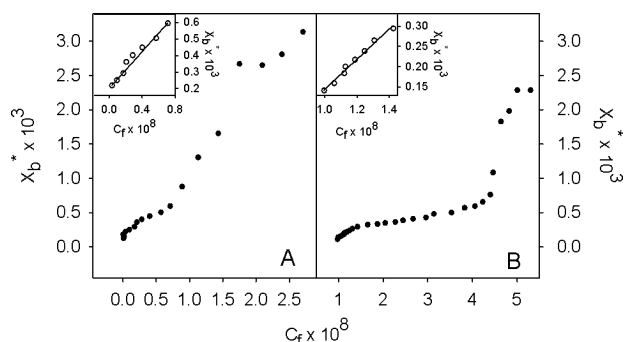


Figure 6. Binding isotherms of NBD-DpreS-his to PG vesicles at pH 5.0 (A) or pH 7.0 (B). From the increments in fluorescence intensity at 530 nm, X_b^* and C_f are calculated as described in Materials and Methods. Partition coefficients were calculated from the initial slope of the corresponding binding isotherm (insets).

behavior. From a threshold concentration of free protein, C_f , a sharp increase in the slope was observed. The partition coefficients, reflecting the binding constants, were calculated as the slopes at the initial intervals (Figure 6, inset), being $1.9 \times 10^4 \text{ M}^{-1}$ and $2.8 \times 10^4 \text{ M}^{-1}$ for pH 7.0 and 5.0 respectively. No partition coefficients could be calculated in the presence of PC.

To study the involvement of a hydrophobic component in the interaction with phospholipids, the effect of DpreS-his on the thermotropic behavior of DMPG and DMPC vesicles was measured by fluorescence depolarization. Liposomes, labeled in the hydrophobic core of the bilayer with the fluorescent probe DPH, were incubated with different DpreS-his concentrations, both at pH 7.0 and pH 5.0. The addition of DpreS-his to DMPG vesicles induced a decrease in the phase transition amplitude in a protein concentration-dependent manner with a minimal variation of 2 $^\circ\text{C}$ of the phase transition temperature (Figure 7). DpreS-his affected almost exclusively the fluorescence polarization values at temperatures above the transition temperature, indicating that the proteins altered mainly the acyl chains in the liquid–crystal phase, inducing a

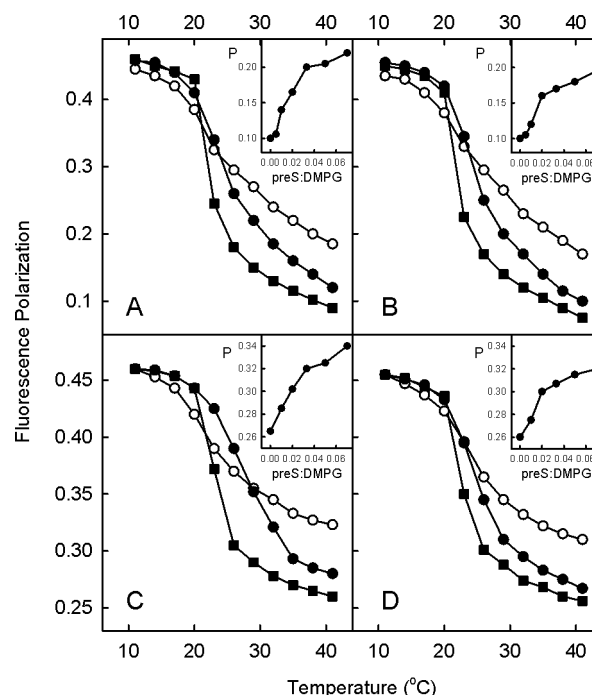


Figure 7. Fluorescence depolarization of DPH-labeled (A and B) and TMA-DPH-labeled (C and D) vesicles with increasing temperatures in the presence of DpreS-his at different protein/lipid molar ratios at pH 5.0 (A and C) and 7.0 (B and D). Phospholipid vesicles (0.14 mM) labeled with DPH (probe/phospholipid weight ratio 500/1) and TMA-DPH (probe/phospholipid weight ratio 100/1) in the absence of protein (■) and incubated with DMPG at a molar protein/phospholipid ratio of 1:100 (●) and 1:20 (○). Insets represent the fluorescence polarization at 37.5 $^\circ\text{C}$ as a function of the protein/lipid molar ratio.

higher order in the chain packing. The presence of DpreS-his up to a molar protein/lipid ratio of 1:20 did not modify neither the transition temperature nor the phase transition amplitude of DMPC vesicles. The fact that only acidic phospholipid vesicles were distorted points to the electrostatic interactions as a crucial determinant of the lipid–protein interaction. As it is observed in the insets of Figure 7, the fluorescence polarization measured at 37.5 $^\circ\text{C}$ increased linearly up to a protein to lipid ratio of 0.02–0.03, remaining almost constant from this point. This value indicates that each molecule of protein prevents the transition phase of approximately 30–50 molecules of phospholipid.

The alteration of the thermotropic behavior of these phospholipids was also studied with the fluorescent probe TMA-DPH. This probe interacts with the polar head of the phospholipids and gives information mainly from the outer monolayer. The results obtained were very similar to those described above for DPH (Figure 7C,D).

Effect of Phospholipid Vesicles on the Secondary Structure of DpreS-his. The circular dichroism spectra of DpreS-his in the presence of PG vesicles are depicted in Figure 8. At pH 5.0 and low phospholipid concentration (up to a protein/lipid ratio of 1:10) there is an increase in the ellipticity value probably due to the aggregation of the protein in the outer layer of the vesicles. At lower protein/lipid ratios, from 1:20 to 1:50, the ellipticity values decreased with a shift of the minimum from 200 to 209 nm and the appearance of a shoulder at 225 nm, characteristic of α -helical structure (Figure 8A). In fact, deconvolution of the CD spectrum by the CCA

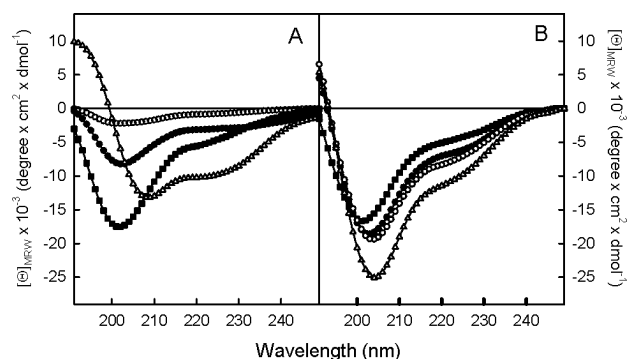


Figure 8. Effect of PG vesicles on the CD spectra of DpreS-his. The spectra were recorded both in the absence (■) and in the presence of PG vesicles, at pH 5.0 (A) and 7.0 (B) after incubating at 37 °C for 1 h. The protein concentration was 0.5 μ M and the protein/lipid molar ratios were 1:5 (●), 1:10 (○), and 1:20 (Δ).

method indicated that the percentage of α helix and β -sheet increased from 4 and 16 to 30 and 33% respectively with the concomitant decrease of nonregular structures (Table 2). In contrast, at pH 7.0 the ellipticity decreased in all cases indicating that aggregation phenomena on the bilayer observed at pH 5.0 are not so important at pH 7.0 (Figure 8B). Furthermore, there is a gradual shift of the minimum to 204 nm and the shoulder at 225 nm is not as obvious as it is at pH 5.0. Deconvolution of CD spectrum by CCA method indicated that the β -sheet structure disappeared increasing the aperiodic component with no change in β -turn. These data indicated a change in the secondary structure of the protein when it interacts with acidic phospholipids and a different behavior at pH 5 and 7. Only at pH 5.0 does the presence of acidic phospholipids induce a conformational change in the protein that increases the α -helix content. On the other hand, the CD spectrum of DpreS-his at pH 5.0 in the presence of PC vesicles at a molar protein/lipid ratio of 1:20 is practically indistinguishable from that shown in Figure 8 in the absence of phospholipid vesicles.

Aggregation, Lipid Mixing, and Release of Contents of Liposomes. The ability of the protein to induce vesicle aggregation was monitored by measuring the variation of the optical density at 360 nm (ΔA_{360}) of a suspension of PG liposomes upon incubation with different DpreS-his concentrations at 37 °C for 1 h. Upon addition of increasing amounts of protein the A_{360} increased until the protein/lipid molar ratio reached a value of 0.017 and 0.042 at pH 7.0 and 5.0 respectively and then remained constant (Figure 9A). The

optical density values reached at pH 5.0 were twice those reached at pH 7.0. On the other hand, DpreS-his did not induce any variation of the optical density of neutral phospholipid vesicles, PC, either at pH 5.0 or pH 7.0. (Figure 9A).

Lipid mixing of phospholipid vesicles was followed by the resonance energy transfer (RET) assay between the fluorescence probes NBD-PE and Rh-PE incorporated into a lipid matrix in which, mixing of phospholipids from labeled and unlabeled liposomes results in a decrease in energy transfer between the fluorescent probes.²⁵ As observed in Figure 9B, DpreS-his domain was able to induce lipid mixing in PG vesicles, both at pH 5.0 and 7.0. Although at low protein/lipid molar ratios, up to a value of 0.014, the decrease of RET was higher at acidic pH, the results obtained at both pH were almost identical when the protein concentration was increased. At both pH values the % RET decreased from 66.5%, in the absence of protein, to 6.5–7.0% at the highest DpreS-his concentration. These values correspond to approximately a 10-fold dilution in the acceptor surface density. Since the mere aggregation of the vesicles would not result in such a change in energy transfer,²⁸ it could be concluded that, under the conditions studied, DpreS-his domains induce the complete fusion of acidic vesicles. However, when neutral phospholipids, PC, were employed DpreS-his did not induce any effect at both pH assayed (Figure 9B).

The ability of DpreS-his to destabilize the lipid bilayer has also been studied by determining the release of aqueous content from phospholipid vesicles, monitored by measuring the increase in ANTS fluorescence at 520 nm.²⁶ As it occurs with aggregation and lipid mixing assays, DpreS-his did not show any effect on PC vesicles neither at pH 5.0 nor at pH 7.0 (Figure 9C). However, the protein induced instability of PG vesicles and was able to induce the release of internal contents of the vesicles in a concentration-dependent manner. The maximum effect was achieved at a protein/lipid molar ratio of 0.06×10^{-2} at pH 5.0 and 0.7×10^{-2} at pH 7.0 (Figure 9C), ratios much lower than those needed to induce vesicle aggregation or lipid mixing. On the other hand, the pH-dependence is higher than that observed in vesicle aggregation or lipid mixing, which could be due to the assay sensitivity or because an aggregation step is needed in order to destabilize the lipid bilayer, the effect being more pronounced at pH 5.0. The maximum fluorescence reached at both pH values, 80–85%, is similar to that described for other proteins and did not attain the value obtained when liposomes were lysed with the detergent Triton X-100 (100% leakage).

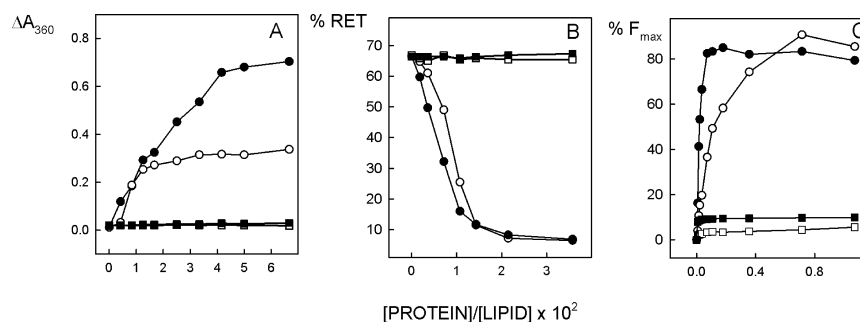


Figure 9. Aggregation (A), lipid mixing (B), and leakage of aqueous content (C) of PG (circles) and PC (squares) vesicles induced by DpreS-his at pH 7.0 (○, □) and 5.0 (●, ■). The final phospholipid concentration was 60 μ M (A) and 0.14 mM (B and C).

DISCUSSION

We have previously shown that the preS domain of HBV is able to interact with and destabilize model membrane systems.¹⁷ In order to extend the studies carried out to other members of the hepadnavirus family, a recombinant DHBV preS protein was obtained with six histidines at the carboxy-terminal end. The strategy employed yielded 15–20 mg of pure and stable protein per liter of culture. Although as a result of the cloning strategy the recombinant protein has another five extra amino acids, it would be expected that 11 residues out of 172 do not promote or modify significantly the interaction of this protein with phospholipid vesicles. At least, the extension of six histidines has no effect on the overall conformation and destabilization properties of HBV preS domains.^{17,22}

The DpreS-his domain, which has an open and mostly nonordered conformation as indicated by fluorescence and circular dichroism spectroscopies, has the ability to interact with acidic phospholipid vesicles. In the presence of negatively charged phospholipids, both at pH 5.0 and 7.0, the maximum of the emission spectrum of NBD-labeled protein shifted to shorter wavelengths, from 548 to 528 nm, which indicates that the region of DpreS-his domain to which NBD moiety is bound, probably the amino terminal end, is located in a more hydrophobic environment. However, the extent of the observed blue shift is lower than that observed with ayw and adr preS subtypes,¹⁷ indicating that penetration of the N-terminal end of DpreS-his into the hydrophobic bilayer is not as deep as that reported for preS subtypes or other pore-forming polypeptides.^{24,29} Binding isotherms provide information about the mechanism of the interaction.³⁰ They showed two different slopes, with a threshold concentration, C_t of 0.7 and 4.5×10^{-8} M at pH 5.0 and 7.0, respectively, at which a sharp increase in the slope was observed. The existence of such a critical concentration could indicate either aggregation of the protein on the surface of the bilayer or the formation of pores with relatively large diameters.²⁴ The partition coefficients, reflecting the binding constants, were on the order of 10^4 M⁻¹, similar to those described for labeled peptides which insert into phospholipid bilayers²⁴ and similar to that obtained with human preS domains.¹⁷ The differences observed between neutral and acidic phospholipids reveal the importance of electrostatic interactions in the binding of the DpreS-his domain to phospholipid vesicles. Only after ionic interaction between the phospholipid polar headgroup and the protein, would the insertion of a region of the latter take place. Moreover, an increase of positive charge as the pH decreases would explain the differences observed between the two pH values.

The results obtained by fluorescence polarization studies corroborate the observed phospholipid specificity since DpreS-his is able to modify the thermotropic behavior of acidic phospholipid vesicles but not that of neutral phospholipids. The decrease of the transition enthalpy together with the small modification of the transition temperature are typical effects of integral membrane proteins.³¹ The insertion of the recombinant protein into the bilayer is stabilized by hydrophobic interaction between the aliphatic chain of the phospholipid and the apolar core of the protein as indicated by the fluorescent probe (DPH), which provides information of the internal area of the bilayer.³² However, an electrostatic interaction component must also exist, as indicated by the fluorescence polarization data obtained with the TMA-DPH probe that

remains anchored to the surface area of the bilayer.³³ When fluorescence polarization data are examined as a function of the protein/lipid ratio, it can be concluded that each molecule of protein prevents the transition phase of approximately 30–50 molecules of phospholipid, suggesting that DpreS-his inserts into the membrane in a more tilted manner than HBV preS which prevents the transition phase of only 20 molecules of phospholipids.¹⁷

Interaction with liposomes also involves structural alteration of the DpreS-his domain. CD spectra indicate the existence of structural changes upon interaction with acidic phospholipids both at pH 7.0 and 5.0. At the latter and at low phospholipid concentration, protein aggregates are formed probably because of an increase in the density of protein on the surface of the bilayer. Such aggregates would produce optical artifacts of differential light scattering and differential absorption flattening and hence an increase in the ellipticity values.³⁴ When the phospholipid concentration increases up to a protein/lipid ratio of 1:20, there is a change in the CD spectrum which must reflect a structural change. This behavior has been described for other proteins which interact with phospholipids, and the conformational change is the result of an increase in the α -helix structure.³⁵ This is the case of ferredoxin in the presence of negatively charged phospholipids,³⁶ which yields a CD spectrum analogous to that obtained for DpreS-his. At pH 7.0, the aggregation does not apparently take place but there is also some conformational change that modifies the CD spectrum. However, the increase in α -helix is not so evident. If we assume that the N-terminal portion of the protein is inserted into the bilayer maintaining the same conformation at both pH values, then the C-terminal end would be the region which increases the helical conformation at pH 5.0 or is able to adopt a nonordered conformation at pH 7.0. However, these data do not allow us to know the conformation that the inserted region adopts. On the other hand, the appearance of either helical or extended conformation as a consequence of the interaction with the bilayer does not determine the acquisition of fusogenic properties since both α -helix and β -sheets have been described as potential fusogenic domains.^{37,38} What seems to be more important in terms of fusogenic propensity is the flexibility that the polypeptide chain possesses, being able to adopt both extended and helical conformations. This is a characteristic feature which has been ascribed to some fusogenic peptides, such as in the case of feline leukemia virus.³⁹ Moreover, the presence of helical and extended structures in the same protein interacting with phospholipids is compatible with their involvement in the fusion process since it has been described that some fusogenic peptides can be divided into two domains, an oblique α -helix inserted in the water–lipid interface, followed by a turn and a β extended structure in the carboxy-terminal end into the hydrophilic phase.⁴⁰

Like HBV preS, DpreS-his domain not only interacts with but it is also able to destabilize membrane model systems. The interaction of the protein with acidic phospholipid vesicles induces their aggregation, as demonstrated by the increase in optical density at 360 nm, higher at pH 5.0 than 7.0. However, these aggregates do not appear when neutral phospholipid vesicles are used which indicates the importance of the electrostatic component on the interaction. In the case of acidic phospholipids, the aggregation leads to fusion, as demonstrated by lipid mixing studies. The maximum value of aggregation and lipid mixing was reached at a protein

concentration of 3–5 μM , respectively, considerable higher than that needed to break the physical integrity of the vesicles, 0.05 μM at pH 5.0. Thus, fusion is not necessary for the release of the aqueous content of the vesicles to take place, just as it occurs with the amino-terminal fusogenic peptide of HIV.⁴¹ The observed dependence of the destabilizing capacity of DpreS-his on both phospholipid composition and pH does not necessarily preclude or determine a particular fusion mechanism. Thus, both neutral and acidic phospholipids have been shown to be specific for the interaction of fusion peptides.^{42,43} On the other hand, and although the membrane destabilizing properties are higher at acidic pH, the fact that all properties are observed at both pHs and that the differences mostly disappear at high protein concentrations, would be in accordance with a pH-independent viral infection model. In the case of viruses infecting cells in a pH-dependent manner, such as influenza virus, no destabilizing effects at neutral pH were observed.⁴⁴

Despite the low similarity of HBV and DHBV preS domains amino acid sequences, only 13 identical amino acids (Figure 10A), both proteins present virtually identical spectroscopic

participates in the fusion of membranes, increasing the activity and adopting a structure in the α -helix on the surface of the membrane while the fusogenic peptide adopts a β -structure,^{48,49} conformations which have been observed for the preS domain and the amino-terminal end of S, respectively.^{13,17}

AUTHOR INFORMATION

Corresponding Author

*Phone: (34) 91 394 42 66. E-mail: pacog@bbm1.ucm.es.

Present Addresses

#ASICI Pabellón Central, Recinto Ferial, 06300 Zafra, Badajoz.

§Janssen-Cilag, S.A., Paseo de las Doce Estrellas, 5–7, 28042 Madrid.

Funding

This work was supported by Grant BFU2010-22014 from the Dirección General de Investigación y Gestión del Programa Nacional I+D+i of the Ministerio de Economía y Competitividad (Spain).

Notes

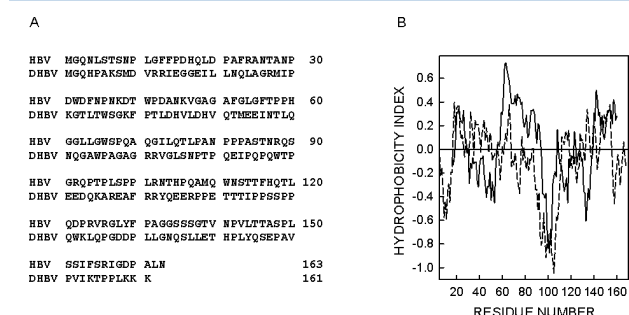
The authors declare no competing financial interest.

ABBREVIATIONS USED

HBV, hepatitis B virus; DHBV, duck hepatitis B virus; DpreS, duck preS domains; PC, egg phosphatidylcholine; PG, phosphatidylglycerol; DMPC, dimyristoylphosphatidylcholine; DMPG, dimyristoylphosphatidylglycerol; NBD-PE, *N*-(7-nitro-2,1,3-benzoxadiazol-4-yl)-dimyristoylphosphatidylethanolamine; Rh-PE, *N*-(lissamine rhodamine B sulfonyl)-diacylphosphatidylethanolamine; ANTS, 8-aminonaphthalene-1,3,6-trisulfonic acid; DPX, *p*-xylenebis(pyridinium) bromide; DPH, 1,6-diphenyl-1,3,5-hexatriene (DPH); TMA-DPH, 1-(4-trimethylammoniumphenyl)-6-phenyl-1,3,5-hexatriene; NBD-F, 4-fluoro-7-nitrobenz-2-oxa-1,3-diazole; CD, circular dichroism; CCA, convex constraint analysis

REFERENCES

- Breiner, K. M., Urban, S., and Schaller, H. (1998) Carboxypeptidase D (gp180), a Golgi-resident protein, functions in the attachment and entry of avian hepatitis B viruses. *J. Virol.* 72, 8098–8104.
- Tong, S., Li, J., and Wands, J. R. (1999) Carboxypeptidase D is an avian hepatitis B virus receptor. *J. Virol.* 73, 8696–8702.
- Li, J., Tong, S., Lee, H. B., Perdigoto, A. L., Spangenberg, H. C., and Wands, J. R. (2004) Glycine decarboxylase mediates a postbinding step in duck hepatitis B virus infection. *J. Virol.* 78, 1873–1881.
- Funk, A., Mhamdi, M., Hohenberg, H., Will, H., and Sirma, H. (2006) pH-independent entry and sequential endosomal sorting are major determinants of hepadnaviral infection in primary hepatocytes. *Hepatology* 44, 685–693.
- Chojnacki, J., Anderson, D. A., and Grgacic, E. V. L. (2005) A hydrophobic domain in the large envelope protein is essential for fusion of duck hepatitis B virus at the late endosome. *J. Virol.* 79, 14945–14955.
- Glebe, D., and Urban, S. (2007) Viral and cellular determinants involved in hepadnaviral entry. *World J. Gastroenterol.* 13, 22–38.
- Zhang, X., Lin, S. M., Chen, T. Y., Liu, M., Ye, F., Chen, Y. R., Shi, L., He, Y. L., Wu, L. X., Zheng, S. Q., Zhao, Y. R., and Zhang, S. L. (2011) Asialoglycoprotein receptor interacts with the preS1 domain of hepatitis B virus in vivo and in vitro. *Arch. Virol.* 156, 637–645.
- Sunyach, C., Rollier, C., Robaczewska, M., Borel, C., Barraïd, L., Kay, A., Trépo, C., Will, H., and Cova, L. (1999) Residues critical for Duck Hepatitis B Virus neutralization are involved in host cell interaction. *J. Virol.* 73, 2569–2575.



- (9) Grgacic, E. V. L., and Anderson, D. A. (2005) S-t, a truncated envelope protein derived from the S protein of duck hepatitis B virus, acts as a chaperone for the folding of the large envelope protein. *J. Virol.* 79, 5346–5352.
- (10) Urban, S., Breiner, K. M., Fehler, F., Klingmüller, U., and Schaller, H. (1998) Avian hepatitis B virus infection is initiated by the interaction of a distinct preS subdomain with the cellular receptor gp180. *J. Virol.* 72, 8089–8097.
- (11) Guo, J. T., and Pugh, J. C. (1997) Topology of the large envelope protein of duck hepatitis B virus suggests a mechanism for membrane translocation during particle morphogenesis. *J. Virol.* 71, 1107–1114.
- (12) Rodríguez-Crespo, I., Núñez, E., Gómez-Gutiérrez, J., Yélamos, B., Albar, J. P., Peterson, D. L., and Gavilanes, F. (1995) Phospholipid interactions of a putative fusion peptide of hepatitis B virus surface antigen S protein. *J. Gen. Virol.* 76, 301–308.
- (13) Rodríguez-Crespo, I., Gómez-Gutiérrez, J., Encinar, J. A., González-Ros, J. M., Albar, J. P., Peterson, D. L., and Gavilanes, F. (1996) Structural properties of the putative fusion peptide of hepatitis B virus upon interaction with phospholipids. Circular dichroism and Fourier-transform infrared spectroscopy studies. *Eur. J. Biochem.* 242, 243–248.
- (14) Rodríguez-Crespo, I., Núñez, E., Yélamos, B., Gómez-Gutiérrez, J., Albar, J. P., Peterson, D. L., and Gavilanes, F. (1999) Fusogenic activity of hepadnavirus peptides corresponding to sequences downstream of the putative cleavage site. *Virology* 261, 133–142.
- (15) Lu, X., Hazboun, T., and Block, T. (2001) Limited proteolysis induces woodchuck hepatitis virus infectivity for human HepG2 cells. *Virus Res.* 73, 27–40.
- (16) Maenz, C., Chang, S. F., Iwanski, A., and Bruns, M. (2007) Entry of duck hepatitis B virus into primary duck liver and kidney cells after discovery of a fusogenic region within the large surface protein. *J. Virol.* 81, 5014–5023.
- (17) Núñez, E., Yélamos, B., Delgado, C., Gómez-Gutiérrez, J., Peterson, D. L., and Gavilanes, F. (2008) Interaction of preS domains of hepatitis B virus with phospholipid vesicles. *Biochim. Biophys. Acta* 1788, 417–424.
- (18) Stoeckl, L., Funk, A., Kopitzki, A., Brandenburg, B., Oess, S., Will, H., Sirma, H., and Hildt, E. (2006) Identification of a structural motif crucial for infectivity of hepatitis B viruses. *Proc. Natl. Acad. Sci. U. S. A.* 103, 6730–6734.
- (19) Blanchet, M., and Sureau, C. (2007) Infectivity determinants of the hepatitis B virus pre-S domain are confined to the N-terminal 75 amino acid residues. *J. Virol.* 81, 5841–5849.
- (20) Gudima, S., Meier, A., Dunbrack, R., Taylor, J., and Bruss, V. (2007) Two potentially important elements of the hepatitis B virus large envelope protein are dispensable for the infectivity of hepatitis delta virus. *J. Virol.* 81, 4343–4347.
- (21) Ni, Y., Sonnabend, J., Seitz, S., and Urban, S. (2010) The pre-s2 domain of the hepatitis B virus is dispensable for infectivity but serves a spacer function for L-protein-connected virus assembly. *J. Virol.* 84, 3879–3888.
- (22) Núñez, E., Wei, X., Delgado, C., Rodríguez-Crespo, I., Yélamos, B., Gómez-Gutiérrez, J., Peterson, D. L., and Gavilanes, F. (2001) Cloning, expression, and purification of histidine-tagged preS domains of hepatitis B virus. *Protein Expr. Purif.* 21, 183–191.
- (23) Perczel, A., Hollósi, M., Tusnády, G., and Fasman, G. D. (1991) Decoupling of the circular dichroism spectra of proteins: The circular dichroism spectra of antiparallel β -sheet in proteins. *Protein Eng.* 4, 669–679.
- (24) Rapaport, D., and Shai, Y. (1991) Interaction of fluorescently labeled pardaxin and its analogues with lipid bilayers. *J. Biol. Chem.* 266, 23769–23775.
- (25) Struck, D. K., Hoekstra, D., and Pagano, R. E. (1981) Use of resonance energy transfer to monitor membrane fusion. *Biochemistry* 20, 4093–4099.
- (26) Ellens, H., Bentz, J., and Szoka, F. C. (1985) H^+ - and Ca^{2+} -induced fusion and destabilization of liposomes. *Biochemistry* 24, 3099–3106.
- (27) Rajarathnam, K., Hochman, J., Schindler, M., and Ferguson-Miller, S. (1989) Synthesis, location, and lateral mobility of fluorescently labeled ubiquinone 10 in mitochondrial and artificial membranes. *Biochemistry* 28, 3168–3176.
- (28) Blumenthal, R., Henkart, M., and Steer, C. J. (1983) Clathrin-induced pH-dependent fusion of phosphatidylcholine vesicles. *J. Biol. Chem.* 258, 3409–3415.
- (29) Rapaport, D., and Shai, Y. (1994) Interaction of fluorescently labeled analogues of the amino-terminal fusion peptide of Sendai virus with phospholipid membranes. *J. Biol. Chem.* 269, 15124–15131.
- (30) Schwarz, G., Gerke, H., Rizzo, V., and Stankowski, S. (1987) Incorporation kinetics in a membrane, studied with the pore-forming peptide alamethicin. *Biophys. J.* 52, 685–692.
- (31) Papahadjopoulos, D., Moscarello, M., Eylar, E. H., and Isac, T. (1975) Effects of proteins on thermotropic phase transitions of phospholipid membranes. *Biochim. Biophys. Acta* 401, 317–335.
- (32) Lentz, B. R., Barenholz, Y., and Thompson, T. E. (1976) Fluorescence depolarization studies of phase transitions and fluidity in phospholipid bilayers. 2 Two-component phosphatidylcholine liposomes. *Biochemistry* 15, 4529–4537.
- (33) Prendergast, F. G., Haugland, R. P., and Callahan, P. J. (1981) 1-[4-(Trimethylamino)phenyl]-6-phenylhexa-1,3,5-triene: synthesis, fluorescence properties, and use as a fluorescence probe of lipid bilayers. *Biochemistry* 20, 7333–7338.
- (34) Mao, D., and Wallace, B. A. (1984) Differential light scattering and absorption flattening optical effects are minimal in the circular dichroism spectra of small unilamellar vesicles. *Biochemistry* 23, 2667–2673.
- (35) Wimley, W. C., and White, S. H. (2000) Designing Transmembrane α -Helices That Insert Spontaneously. *Biochemistry* 39, 4432–4442.
- (36) Horniak, L., Pilon, M., van 't Hof, R., and de Kruijff, B. (1993) The secondary structure of the ferredoxin transit sequence is modulated by its interaction with negatively charged lipids. *FEBS Lett.* 334, 241–246.
- (37) Bullough, P. A., Hughson, F. M., Skehel, J. J., and Wiley, D. C. (1994) Structure of influenza haemagglutinin at the pH of membrane fusion. *Nature* 371, 37–43.
- (38) Nieva, J. L., Nir, S., and Wilschut, J. (1998) Destabilization and fusion of zwitterionic large unilamellar lipid vesicles induced by a β -type structure of the HIV-1 fusion peptide. *J. Liposome Res.* 8, 165–182.
- (39) Davies, S. M., Epand, R. F., Bradshaw, J. P., and Epand, R. M. (1998) Modulation of lipid polymorphism by the feline leukemia virus fusion peptide: implications for the fusion mechanism. *Biochemistry* 37, 5720–5729.
- (40) Callebaut, I., Tasso, A., Brasseur, R., Burny, A., Portetelle, D., and Mornon, J. P. (1994) Common prevalence of alanine and glycine in mobile reactive centre loops of serpins and viral fusion peptides: do prions possess a fusion peptide? *J. Comput. Aided Mol. Des.* 8, 175–191.
- (41) Nir, S., and Nieva, J. L. (2000) Interactions of peptides with liposomes: pore formation and fusion. *Prog. Lipid Res.* 39, 181–206.
- (42) Duzgunes, N., and Shavnin, S. A. (1992) Membrane destabilization by N-terminal peptides of viral envelope proteins. *J. Membr. Biol.* 128, 71–80.
- (43) Samuel, O., and Shai, Y. (2001) Participation of two fusion peptides in measles virus-induced membrane fusion: emerging similarity with other paramyxoviruses. *Biochemistry* 40, 1340–1349.
- (44) Stegmann, T., Hoekstra, D., Scherphof, G., and Wilschut, J. (1986) Fusion activity of influenza virus. A comparison between biological and artificial target membrane vesicles. *J. Biol. Chem.* 261, 10966–10969.
- (45) Lavillette, D., Pecher, E. I., Donot, P., Fresquet, J., Molle, J., Corbau, R., Dreux, M., Penin, F., and Cosset, F. L. (2007) Characterization of fusion determinants points to the involvement of three discrete regions of both E1 and E2 glycoproteins in the membrane fusion process of hepatitis C virus. *J. Virol.* 81, 8752–8765.

- (46) Pacheco, B., Gómez-Gutiérrez, J., Yélamos, B., Delgado, C., Roncal, F., Albar, J. P., Peterson, D., and Gavilanes, F. (2006) Membrane-perturbing properties of three peptides corresponding to the ectodomain of hepatitis C virus E2 envelope protein. *Biochim. Biophys. Acta* 1758, 755–763.
- (47) Pérez-Berna, A. J., Guillén, J., Moreno, M. R., Gómez-Sánchez, A. I., Pabst, G., Laggner, P., and Villalain, J. (2008) Interaction of the most membranotropic region of the HCV E2 envelope glycoprotein with membranes. Biophysical characterization. *Biophys. J.* 94, 4737–4750.
- (48) Gray, C., Tatulian, S. A., Wharton, S. A., and Tamm, L. K. (1996) Effect of the N-terminal glycine on the secondary structure, orientation, and interaction of the influenza hemagglutinin fusion peptide with lipid bilayers. *Biophys. J.* 70, 2275–2286.
- (49) Peisajovich, S. G., Epand, R. F., Pritsker, M., Shai, Y., and Epand, R. M. (2000) The polar region consecutive to the HIV fusion peptide participates in membrane fusion. *Biochemistry* 39, 1826–1833.
- (50) Eisenberg, D., Schwarz, E., Komaromy, M., and Wall, R. (1984) Analysis of membrane and surface protein sequences with the hydrophobic moment plot. *J. Mol. Biol.* 179, 125–142.